# [AMT 11] Effect of Dy doping on the properties of La-Ca-Mn-O ceramics

**Sharmiwati Mohd Sharif, Abdul Halim Shaari, Lim Kean Pah, Kabashi Kathir Kabashi, Abdullah Chik, Wan Mahmood Mat Yunus, Hishamuddin Zainuddin**

Superconductor and Thin Film Laboratory, Department of Physics, Faculty of Science and Environmental Studies, Universiti Putra Malaysia, 43400 Serdang, Selangor.

## Introduction

The discovery of colossal magnetoresistance (CMR) has received attention since 1950s. As the name applies, these materials show huge change in electrical resistivity with the applied magnetic field. The CMR material usually described with the formula $Ln_{1-x}A_xMnO_3$ where Ln usually the trivalent rare earth ions ($La^{3+}$, $Pr^{3+}$, $Nd^{3+}$, etc.) and A is the divalent ions ($Ca^{2+}$, $Ba^{2+}$, $Sr^{2+}$). It is commonly found that the CMR material has a temperature-dependent behavior of resistance at zero-field and the largest CMR effect appears at insulator-metal (I-M) transition. The traditional understanding of CMR effect is generally based on the double exchange (DE) mechanism. However, the DE mechanism alone could not account for the observed transport properties and other effects found such as charge-ordering transition due to the long range Coulomb interaction among the carriers, electron phonon coupling arising from the Jahn-Teller distortion of $Mn^{3+}$ etc.

The influences of Dy doping in La site of $(La_{1-x}Dy_x)_{7/8}Ca_{1/8}MnO_3$, $(La_{1-x}Dy_x)_{2/3}Ca_{1/3}MnO_3$ and $(La_{1-x}Dy_x)_{1/2}Ca_{1/2}MnO_3$ systems have been studied. The doping concentration were varied in a full range from x=0.00 to x=1.00 for each system.

## Materials and methods

The raw materials for the experiment are reagent grade $La_2O_3$, $Dy_2O_3$, $CaCO_3$ and $MnO_3$ in powder form. The synthesis was performed by solid state reaction method where the powders were mixed and milled together for 6 hours and dried in the oven overnight. The dried mixture was calcined at 900°C for 12 hours at the rate of 3°C per minute. The calcine products were then sintered at 1300°C for 24 hours at rate of 2°C per minute with several intermediate grindings and pelletizations.

The properties of the samples were investigated using various instruments available at our Superconductor and Thin Film laboratory and other UPM facilities. Structure properties were studied by using an X-ray diffractometer (XRD) at room temperature on compacted powder samples and the microstructure studies were using Scanning Electron Microscope (SEM). The resistance measurements were performed over the temperature ranges 20-300K on all the samples using the standard four-point probe measurement system. The magnetic properties were studied via AC susceptibility (ACS) measurements using a Lakeshore AC Susceptometer (model 7000). Magnetoresistance (MR) measurement was performed by a conventional four-point probe method with applied external magnetic field. By varying the magnetic field up to 1 Tesla, which is supplied by the power supply to the magnetic coil, a series of resistance change with different magnetic fields are obtained and at constant temperatures of 100 K, 150 K, 170 K, 200 K and 250 K with magnetic field varying from 0T to 1T respectively. The magnetoresistance effect was then obtained by using the equation. The data was collected manually.

## Results

XRD data show that the samples of each system are in orthorhombic distorted perovskite structures, which resulted from the JT distortion. This lattice distortion weakens the DE coupling among the Mn ions and breaks the path of the electron hopping. The evolution of the cell volume and lattice parameters for $(La_{1-x}Dy_x)_{7/8}Ca_{1/8}MnO_3$ system are displayed in figure 1. The continuous unit-cell volume decrease along the series is due to the smaller size of the $Dy^{3+}$ (x=0.5). As the doping increase from x=0.75 to x=1.00, the unit-cell volume increase as the $Dy^{3+}$ take place from La site. While b and c decrease continuously with the Dy concentrations, the parameter a shows an increase. This change in the behaviour of parameter a is characteristic of

perovskites with high orthorhombic distortion, such as reports in literature (Blasco *et al*., 1996). According to (Li *et al*., 1998), the orbital degeneracy leads to a Jahn-Teller instability, which causes the oxygen octahedral to distort and lower its site symmetry to tetragonal or orthorhombic and thus removing orbital degeneracy. This distortion increases the Mn-O distance and the Mn-O-Mn angle, which leads to the decrease of the DE interactions between Mn ions.

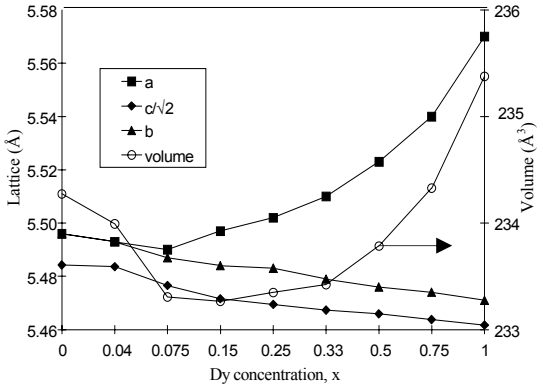


FIGURE 1 The evolution of the cell volume and lattice parameters for $(La\text{-}Dy)_{7/8}Ca_{1/8}MnO_3$ system.

The evolution of the cell volume and lattice parameters for are displayed in figure 2.

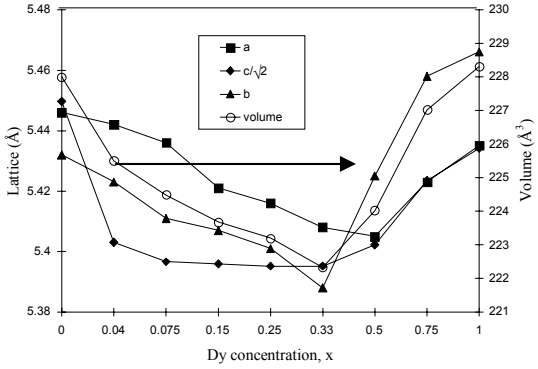


FIGURE 2 The evolution of the cell volume and lattice parameters for $(La\text{-}Dy)_{2/3}Ca_{1/3}MnO_3$ systems.

The continuous unit-cell volume decrease along the series is due to the smaller size of the $Dy^{3+}$ (x=0.33). As the doping increase from x=0.5 to x=1.00, the unit-cell volume increase as the $Dy^{3+}$ take place from La site. That is the reasons to what had happen to the unusual phases which is appear in XRD patterns. However, all the samples are in orthorhombic form of perovskite structure. As referred to (Blasco *et al*., 1996), the lattice parameters of $La_{2/3}Ca_{1/3}MnO_3$ are a=5.47 Å, b=5.46Å and c=7.71 Å. Hence, this system has orthorhombic distorted perovskite structure. For instance, $a>b\approx c/\sqrt{2}$ for $La_{2/3}Ca_{1/3}MnO_3$ and samples with low Dy concentrations orthorhombic distortion while $b>a>c/\sqrt{2}$ for $Dy_{2/3}Ca_{1/3}MnO_3$, with higher orthorhombic distortion. This distortion increases the Mn-O distance and the Mn-O-Mn angle, which leads to the decreases of the DE interactions between Mn ions.

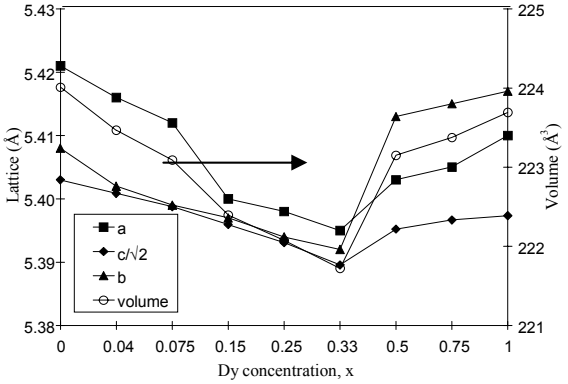


FIGURE 3 The evolution of the cell volume and lattice parameters for $(La\text{-}Dy)_{1/2}Ca_{1/2}MnO_3$ system.

The evolution of the cell volume and lattice parameters are calculated and displayed in figure 3. The continuous unit-cell volume decrease along the series is due to the smaller size of the $Dy^{3+}$ (x=0.33). As the doping increase from x=0.5 to x=1.00, the unit-cell volume increase as the Dy take place from La site. However, all the samples are still in orthorhombic form of perovskite structure. As referred to (Rajappan *et al*., 1998), the lattice parameters of $La_{1/2}Ca_{1/2}MnO_3$ are a=5.434 Å, b=5.413 Å and c=7.649 Å and the system in orthorhombic distorted perovskite structure and the value of each lattice parameter is closely to the experimental ones. For instance, $a>b\approx c/\sqrt{2}$ for $La_{1/2}Ca_{1/2}MnO_3$ and samples with low Dy concentrations orthorhombic distortion while $b>a>c/\sqrt{2}$ for high Dy concentrations and $Dy_{1/2}Ca_{1/2}MnO_3$, with higher orthorhombic distortion. This distortion increases the Mn-O distance and the Mn-O-Mn angle, which leads to the decreases of the DE interactions between Mn ions. As mentioned in (Li *et al*., 2001), the introduction of other ions in this system causes local lattice distortions due to its ionic radius.

From the susceptibility measurement as a function of $(La\text{-}Dy)_{7/8}Ca_{1/8}MnO_3$ compound undergoes the typical transition from the paramagnetic to ferromagnetic insulator. The second transition is to an antiferromagnetic phase with a possible charge-ordering process (Castro *et al*., 1999).

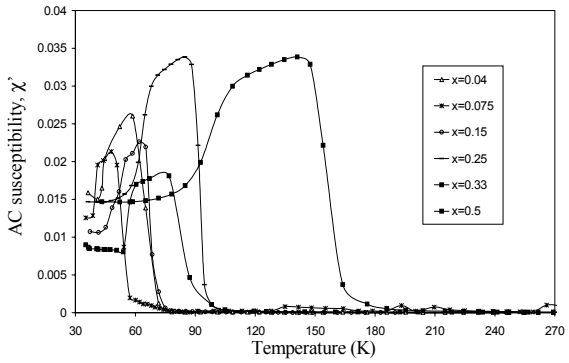


FIGURE 4 Magnetic AC susceptibility of $(La_{1-x}Dy_x)_{7/8}Ca_{1/8}MnO_3$ for x=0.04, x=0.075, x=0.15, x=0.25 and x=0.33 at 1.0 Oe.

For the $(La\text{-}Dy)_{2/3}Ca_{1/3}MnO_3$ system, all samples with Dy content show a clear deviation from the well behaved ferromagnetic behaviour seen for the undoped sample. In a well-behaved ferromagnet, the spontaneous magnetization is well represented by the saturation magnetization. However, in systems where spins are canted, the applied magnetic field may suppress the domain wall but it could simultaneously align the spins on microscopic length scale, so that the internal magnetization increases with the applied field.

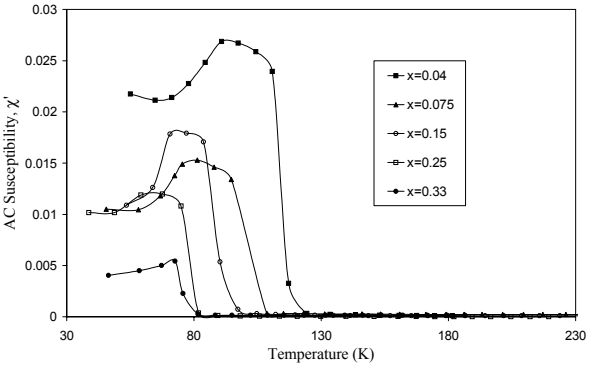


FIGURE 5 Magnetic AC susceptibility of $(La_{1-x}Dy_x)_{2/3}Ca_{1/3}MnO_3$ for x=0.04, 0.075, 0.15, 0.25 and 0.33 at 1.0 Oe.

The $(La\text{-}Dy)_{1/2}Ca_{1/2}MnO_3$ system shows both ferromagnetic and antiferromagnetic transition in agreement with those in literature (Babu *et al*., 2001). But, the presence of charge-ordering has also been observed in undoped sample by Babu *et al*. (2001). The presence of Dy in the system, disturbed the antiferromagnetic and another phase appears at a much lower temperature. Similiarly, Castro et al., (1999) reported that the enhancement in the axial bond angle on yttrium substitution in lanthanum site reduce the antiferromagnetic coupling.

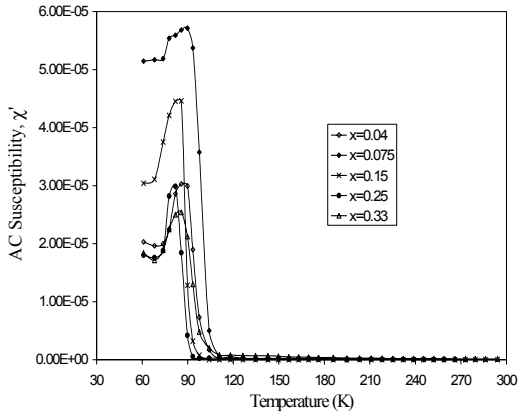


FIGURE 6 Magnetic AC susceptibility of $(La_{1-x}Dy_x)_{1/2}Ca_{1/2}MnO_3$ for x=0.04 to x=0.33 at 1.0 Oe.

From the resistance measurement, all the samples of three systems exhibit maximum resistance at $T_P$ which indicate the transition from metallic-like behaviour to insulator behaviour upon warming the samples to room temperature. Phase transition temperature, $T_P$ of $(La\text{-}Dy)_{7/8}Ca_{1/8}MnO_3$, $(La\text{-}Dy)_{2/3}Ca_{1/3}MnO_3$ and $(La\text{-}Dy)_{1/2}Ca_{1/2}MnO_3$ systems are as shown in figure 7.

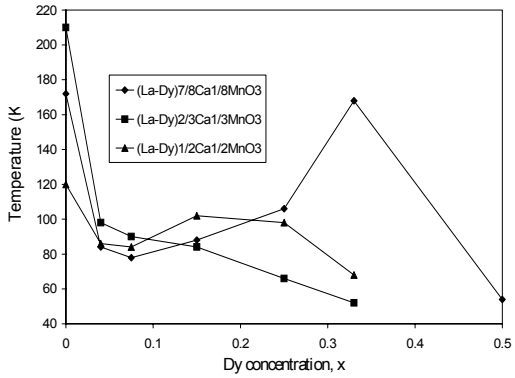


FIGURE 7 $T_P$ of $(La\text{-}Dy)_{7/8}Ca_{1/8}MnO_3$, $(La\text{-}Dy)_{2/3}Ca_{1/3}MnO_3$ and $(La\text{-}Dy)_{1/2}Ca_{1/2}MnO_3$ systems as a function of Dy concentration.

$T_P$ of $(La\text{-}Dy)_{2/3}Ca_{1/3}MnO_3$ and $(La\text{-}Dy)_{1/2}Ca_{1/2}MnO_3$ systems show linearly decrease as compared to that $(La\text{-}Dy)_{7/8}Ca_{1/8}MnO_3$ systems. The $T_P$ of (La-

$Dy)_{7/8}Ca_{1/8}MnO_3$ up to doping level of x=0.33. Further doping, the $T_P$ decrease linearly. For $(La\text{-}Dy)_{1/2}Ca_{1/2}MnO_3$ systems, the $T_P$ decrease as Dy exist but for further doping to x=0.15, the $T_P$ are increase. For the higher doping up to x=0.5, the $T_P$ decrease linearly as the Dy content increase. As a result, concentration of $Dy^{3+}$ (x=0.33) enhance the $T_P$ in $(La\text{-}Dy)_{7/8}Ca_{1/8}MnO_3$ as compared to other systems.

The semiconductor model ln(R) α ($-E_a/k_BT$) was used to explain the transport mechanism of the perovskite manganites above $T_P$. The values of activation energy are in the order of 0.2 eV or lower for all samples of $(La\text{-}Dy)_{7/8}Ca_{1/8}MnO_3$, $(La\text{-}Dy)_{2/3}Ca_{1/3}MnO_3$ and $(La\text{-}Dy)_{1/2}Ca_{1/2}MnO_3$ systems, indicating that these samples exhibit narrow band-gap semiconducting compounds.

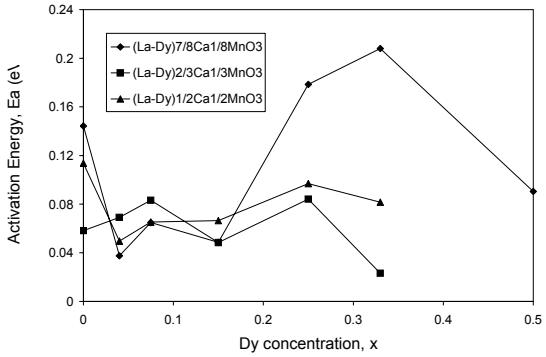


FIGURE 8 $E_a$ of $(La\text{-}Dy)_{7/8}Ca_{1/8}MnO_3$, $(La\text{-}Dy)_{2/3}Ca_{1/3}MnO_3$ and $(La\text{-}Dy)_{1/2}Ca_{1/2}MnO_3$ systems as a function of Dy concentration.

Phase diagram deduced from $T_C$ and $T_P$ correlate a close interplay between magnetism and transport properties, via a DE mechanism of $Mn^{3+}$-O-$Mn^{4+}$ as suggested by Zener. However, the substitution of Dy in these three systems favour the DE interaction up to x=0.3. Beyond this composition, $T_C$ and $T_P$ deviates indicating the decrease in the long-range ferromagnetism and metallic conductivity.

By totally replacing La with Dy in the systems, CMR values were also observed at temperature approaching their $T_P$. The CMR values of $(La\text{-}Dy)_{7/8}Ca_{1/8}MnO_3$, $(La\text{-}Dy)_{2/3}Ca_{1/3}MnO_3$ and $(La\text{-}Dy)_{1/2}Ca_{1/2}MnO_3$ systems are very temperature dependent. Each of the samples exhibits the maximum value of CMR at certain temperature and for these three systems, the value observed is near to its $T_P$. The maximum value of CMR for each doping level of $(La\text{-}Dy)_{7/8}Ca_{1/8}MnO_3$, $(La\text{-}Dy)_{2/3}Ca_{1/3}MnO_3$ and $(La\text{-}Dy)_{1/2}Ca_{1/2}MnO_3$ systems are plotted in figure 9. For the undoped sample, the maximum CMR value observed is 57.4% for $(La\text{-}Dy)_{2/3}Ca_{1/3}MnO_3$ system. Among these three systems, the highest value of CMR as the Dy exist is observed for $(La\text{-}Dy)_{7/8}Ca_{1/8}MnO_3$ system with x=0.33 in value of 56.9%.

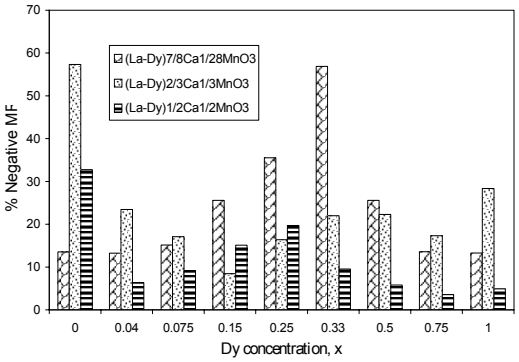


FIGURE 9 The percentage of MR of $(La\text{-}Dy)_{7/8}Ca_{1/8}MnO_3$, $(La\text{-}Dy)_{2/3}Ca_{1/3}MnO_3$ and $(La\text{-}Dy)_{1/2}Ca_{1/2}MnO_3$ systems as a function of Dy concentration.

**Discussion**

In conclusion, when $La^{3+}$ (ionic radius: 1.216 Å) is replaced with a smaller Dy ion (ionic radius: 1.083Å) the $MnO_6$ octahedra buckled. Since $Dy^{3+}$ replaces $La^{3+}$, doping with Dy is expected to leave the $Mn^{3+}$:$Mn^{4+}$ ratio unchanged. In the electron hopping mechanism since only the Mn electrons hopping is active, the motion of the charge carriers and hence the conductivity of the material is expected to be largely controlled by the geometric arrangement of the ions. Also the buckling of $MnO_6$ octahedra, in turn giving rise to weaker DE interaction, can be expected to result in the reduction of ferromagnetic exchange and metallic conduction. Since the ferromagnetic interactions compete with coexisting superexchange antiferromagnetic interactions and also with the possible antiferromagnetism interaction between the rare earth and Mn ions, the system is driven towards a spin glass or local spin canted arrangement. It is observed that although $Dy^{3+}$ is a magnetic material; it does not enhance the ferromagnetism.

**Acknowledgements**

The authors wished to thank the Ministry of Science, Technology and Innovation (MOSTI), Malaysia for the National Science Fellowship awarded to Sharmiwati Mohd. Sharif and IRPA grant awarded to Prof. Dr Abdul Halim Shaari.

**References**

Babu, P. D., Das, A. and Paranjpe, S. K. (2001). Effect of yttrium substitution in charge ordered antiferromagnetic $La_{0.5}Ca_{0.5}MnO_3$. *Solid State Communications*, 118, 91-95.

Blasco, J., García J., de Teresa, J. M., Ibarra, M. R., Algarabel, P. A. and Marquina C. (1996). A systematic study of structural, magnetic & electrical properties of $(La_{1-x}Tb_x)_{2/3}Ca_{1/3}MnO_3$ perovskite. *Journal Physics: Condens Matter*, 8(40), 7427-7442.

Castro, M., Burriel, R. and Cheong, S. W. (1999). Magnetic and heat-capacity anomalies of $La_{7/8}Ca_{1/8}MnO_3$. *Journal of Magnetism and Magnetic Materials*, 196-197, 512-514.

Li, R-W., Sun, J-R., Wang, Z-H., Zhang, S-Y and Shen, B-S. (2000). Magnetic and transport properties of Sn-doped $La_{0.5}Ca_{0.5}MnO_3$. *J. Phys. D: Appl. Phys*., 33, 1982-1984.